Imec's large-area n-PERT cells: Raising the efficiency beyond 22% by selective laser doping

Monica Aleman, Angel Uruena, Emanuele Cornagliotti, Aashish Sharma, Richard Russell, Filip Duerinckx & Jozef Szlufcik, imec, Leuven, Belgium

ABSTRACT

This paper presents the main features of imec's n-PERT (passivated emitter rear totally diffused) cells, which have achieved independently confirmed efficiencies of 22%. A special focus is given to the selective front-surface field formation by laser doping, which – combined with imec's front-plating sequence and the excellent rear-surface passivation by Al_2O_3 on the boron-diffused emitters – has enabled very high voltages (close to 685mV) to be realized on large-area n-type Cz material.

Introduction

The PV module market is currently dominated by standard screen-printed aluminium back-surface field (Al-BSF) silicon solar cells, which represent about 90% of total silicon solar cell production. Although their fabrication is simple and robust, there is a downside in that the typical conversion efficiency of Al-BSF cells is limited to values of around 19% as a result of various technological limitations, including:

- Strong Auger recombination at the front junction, because of the high surface doping level required by the screen-printing pastes for good electrical contact.
- Reduced optical response on the rear, because of parasitic absorption in the metal.
- Poor passivation of the Al-BSF on the rear side.

These cells also suffer from wafer bowing due to the different thermal expansion coefficients of silicon and aluminium.

> "Typical conversion efficiency of Al-BSF cells is limited to values of around 19%."

With the continuous fall in module prices and the increasing influence of the balance of system cost on the levelized cost of electricity (LCOE), there is a growing desire for high-efficiency modules – hence the worldwide interest in passivated emitter and rear cell (PERC) technology, which enables higher efficiencies than Al-BSF cells to be achieved. PERC cells use dielectrics on the rear side, improving both the rear passivation and the optical response. The electrical contacts are locally formed by opening small areas in the dielectrics. Industrial manufacturing of PERC cells on p-type material has already been in place for several years at companies such as Sunrise and Hanwha Q CELLS. Although Schott Solar have shown efficiencies of up to 21% to be achievable on large-area devices [1], an average of 20.4% is expected for the high-volume production by Trina Solar [2]. Passivated emitter and rear locally diffused (PERL) and passivated emitter rear totally diffused (PERT) structures are also of great interest in R&D: whereas the first enables even higher efficiencies (up to 25% on a lab scale), the second can be produced using current production lines without introducing too many changes.

At imec a process flow is under development with which we have already achieved 22% efficiency with

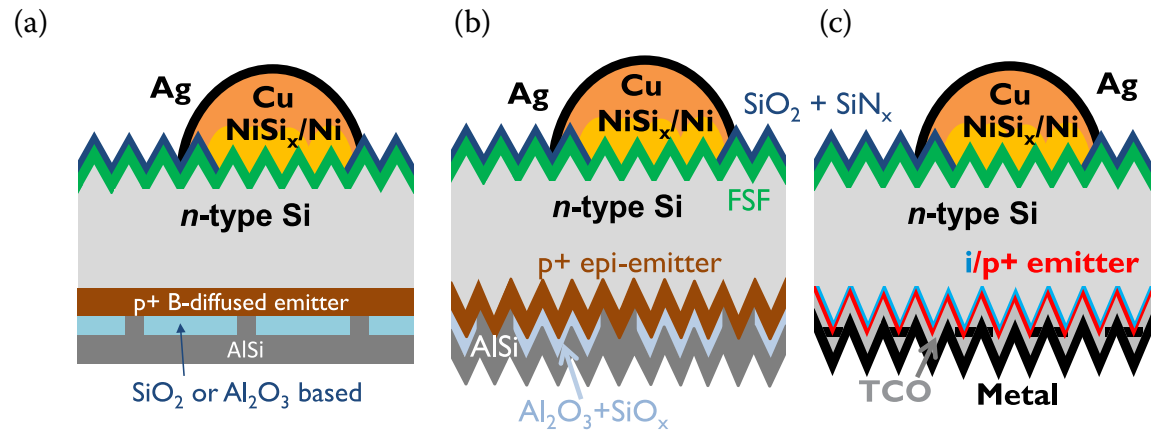

Figure 1. Schematics of n-Si rear-junction concepts under study at imec: (a) diffusion route; (b) epitaxial route; (c) hybrid route.

large-area, back-junction n-PERT cells. This research activity began by combining the best of imec's p-type PERC and n-type IBC platforms. For the front-side metallization of n^+ surfaces from the p-type PERC platform, imec's know-how was put to use in laser patterning and plating. The high-quality rear-junction formation by boron diffusion and the rear passivation by thermal oxidation on n-type substrates originated from the IBC platform.

Fig. 1(a) shows a schematic of imec's first devices, which are constructed on large-area, commercially available, n-type Cz-Si wafers with a typical base resistivity in the range 3–5Ωcm. The front surface is textured with random pyramids formed in an alkaline solution. Minority carriers are shielded from the front surface by a diffused front-surface field (FSF), which is passivated by a thin thermal oxide coated with a plasma-enhanced chemical vapour deposition (PECVD) silicon nitride as an anti-reflection coating (ARC). Contact openings on the front are created by laser ablation, followed by a Ni/Cu/Ag plating sequence.

On the rear side, three different process flows are evaluated; the flows differ in the methods used to fabricate the p^+ junction. The diffused baseline, which acts as a reference (see Fig. 1(a)), relies on BBr_3 diffusion to create the rear emitter and on dielectric passivation, based on either a thermal SiO_2 or an Al_2O_3/SiO_x coating. Laser ablation is used to define the rear-contact pattern, while physical vapour deposition (PVD) by sputtering of Al is used to form the back-side contact.

Another flow consists of the epitaxial growth of the rear emitter (Fig. 1(b)). This route allows a simplified process sequence and more freedom in the design of the emitter doping profile, resulting in very low emitter dark saturation current densities (J_{0e}). More information for this cell type can be found in Recaman et al. [3].

The final flow makes use of an a-Si i/p^+ heterojunction emitter (Fig. 1(c)), thereby enabling a 1D current flow on the rear surface with excellent J_{0e} values due to the passivated contact structure. More details can be found in Tous et al. [4].

This paper will concentrate more on the characterization and cell results obtained for the diffused emitter route, although all details relating to the front-surface optimization are equally applicable to the other process flows, since they all share the front-side processing.

Features of imec's n-PERT cells

Material

The choice of phosphorus-doped Cz wafers has several advantages. The bulk of this material is less sensitive than p-type wafers to iron and other metallic impurities. For many common metallic impurities, the capture cross section for electrons is greater than that for holes. The smaller capture cross section for n-type substrates results in a higher bulk lifetime (and longer diffusion length). Additionally, phosphorus-doped wafers do not suffer from the light-induced degradation typically observed with boron-doped substrates. Moreover, even though the current price of n-type Si is higher than for p-type Si, it is expected that, with the increase in n-type Si production, prices will even out because of economies of scale. This is expected to happen, as the International Technology Roadmap for Photovoltaics (ITRPV) predicts an increase in the share of n-type Si wafers in the market, mainly for high-efficiency devices [5].

A potential disadvantage of cells based on n-type silicon wafers, grown with the standard Czochralski method, is the wide resistivity range found in a typical phosphorus-doped ingot (due to the low segregation coefficient of phosphorus in silicon). Although imec's n-PERT devices typically use 3–5Ωcm material, dedicated experiments have shown that similar efficiencies (±0.1%) are obtainable for base resistivities in the range 2–10Ωcm, with small but opposite trends for the short-circuit current and the open-circuit voltage as a function of the base resistivity.

Front contacts

As mentioned earlier, plating is applied for the front-side metallization; this enables a self-aligned contact formation, where the metal is selectively deposited in the laser-patterned areas. The plating sequence for the front side is as follows. First, a light-induced plating (LIP) step is performed for nickel and copper deposition. Ni is used to improve the contact formation to the FSF and to protect the wafer from Cu diffusion. Next, copper electroplating is carried out to increase the finger thickness, so that a higher line conductivity can be achieved. The contacts are finally finished with a very thin 'flash' Ag coating (~100nm) to prevent copper oxidation. All these steps are performed in a single inline plating tool.

A metallization scheme based on copper plating has several advantages. First of all, copper prices per kilo equate to only 1% of Ag prices and are less susceptible to fluctuation; the influence on the final cell/module price is therefore much smaller. The features of the plated fingers are also narrower than those of printed cells (enabling more light to come into the device). Moreover, the use of Ni facilitates the contact formation in areas with a surface doping concentration as low as $10^{19}cm^{-3}$, which is an order of magnitude smaller than the surface doping concentration typically required by standard screen-printing pastes. The implementation of such lightly doped profiles on the front represents an improved spectral response (particularly for the short-wavelength region), because of the lower Auger recombination in the diffused FSF, which has a favourable effect on both the current and the voltage. In addition, the response in the IR region of the spectrum is improved as well, because of a reduction in free-carrier recombination (FCA) due to the lower doping of the FSF. In other words, the use of nickel-plated contacts for the front metallization allows higher voltages and currents to be achieved for two-side contacted cells.

Rear junction

A rear-junction device presents several advantages over the front-junction cells on n-type material:

- The front side can be easily contacted with a well-developed metallization process based on Ni/Cu plating on n^+ surfaces patterned by laser ablation. The cell layout (n^+ front/p^+ rear) is the same as that for current p-type PERC cells, enabling it to be adopted by industry more quickly.
- There is a negligible impact on cell performance because of the retrograde boron profile (compared with a front-junction cell).
- Since the bulk has the same polarity as the FSF, it also contributes to the majority-carrier flow on the front. The front design can be further optimized while still keeping the same lateral resistance: either the number of front fingers compared with a front-junction device (see Fig. 2) is reduced (which would lower the shadowing and recombination losses), or the total front doping concentration is reduced (which would also reduce the front recombination).

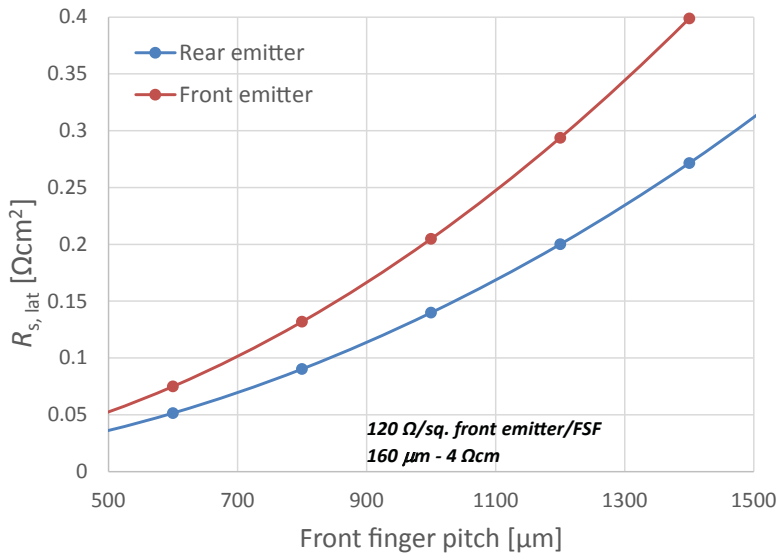

Figure 2. Simulation of the lateral series resistance as a function of the front pitch for front-junction and rear-junction cells. For the simulation a 160µm-thick cell on 4Ωcm material with a front FSF/emitter doping of 120Ω/sq. was assumed [6].

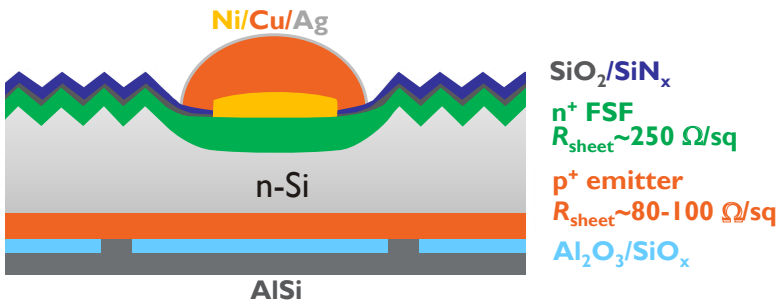

Figure 3. Schematic of imec's n-PERT cell, featuring a laser-doped and plated FSF, and a boron-diffused emitter and Al_2O_3/SiO_x dielectric stack on the rear. Record efficiencies of up to 22% have been demonstrated with this cell.

Rear passivation

In the first imec devices the rear-side passivation was delivered by a ~100nm-thick thermal oxide layer grown during a wet-oxidation step. J_0 values of 25–30fA/cm² were achieved on the standard boron-diffused emitter, featuring a sheet resistance between 90 and 100Ω/sq.

It has already been shown that Al_2O_3 layers result in lower saturation current densities than thermal oxide passivation [7]. With the replacement of the silicon oxide passivation by an aluminium oxide layer, the passivated $J_{0,rear}$ goes down to 14fA/cm² [6]. The thin Al_2O_3 coating is capped with a PECVD SiO_x layer to improve the rear optical response [8]; the PECVD deposition of the SiO_x does not, however, have any detrimental impact on the passivation quality of the Al_2O_3. For more information on this subject see Cornagliotti et al. [6].

Front-surface field

Most of the carrier generation occurs on the front side. The minority carriers have to travel through the wafer thickness to reach the rear junction; consequently, these devices are very sensitive to the front-surface recombination. An optimal FSF needs to deliver a good shield against Shockley-Read-Hall recombination while fulfilling two different conditions: a light doping on the non-contacted areas in order to keep the Auger recombination as low as possible, and a deep, heavily doped profile on the contacted area in order to achieve a good and well-passivated electrical contact.

A single diffused FSF (R_{sheet} ≈ 120Ω/sq.) was first implemented. To enable a good electrical contact with nickel, and avoid a heavily doped surface, a compromise in the profile design had to be made; passivated J_0 values are around 50fA/cm² for this profile. The impact of the laser-ablation process on the front-side recombination was characterized, and it was observed that shallower junctions suffer from a stronger laser-induced degradation [9]. For imec's process in particular, this resulted in a $J_{0,laser}$ greater than 5000fA/cm² – in other words, a total front recombination $J_{0,front}$ greater than 100fA/cm² after the laser treatment, with an implied V_{oc} of around 668mV (assuming a J_{sc} of 39.5mA/cm²).

> "Selective laser doping is an excellent technological alternative, with strong potential for forming local junctions in industrial environments."

Selective laser doping

To overcome FSF limitations, a more sophisticated front design based on the selective junction formation by laser doping was developed and implemented in imec's process flow (Fig. 3). Selective laser doping is an excellent technological alternative, with strong potential for forming local junctions in industrial environments. A commercial spin-on dopant (SOD) is spin coated over a surface, and a deep junction is formed through quasi-continuous wave laser doping. In imec's devices a phosphorus-containing SOD is applied on top of the silicon nitride ARC to create an n^{++}-doped area, during which narrow lines ~10µm wide and over 2µm deep are locally formed. The profile characteristics depend on the laser power and speed [10].

As can be seen in Fig. 4, the front-side pyramids are flattened during laser doping; this behaviour is not observed for laser-ablated samples. The SOD residues are removed in a short HF dip. The laser damage generated during laser doping is subsequently annealed in a belt furnace anneal (BFA) [11]; this anneal also enables the formation of a good electrical contact on the rear and the passivation of the different doped regions [12].

After the BFA, the cells are plated following the sequence presented earlier. The use of selective laser

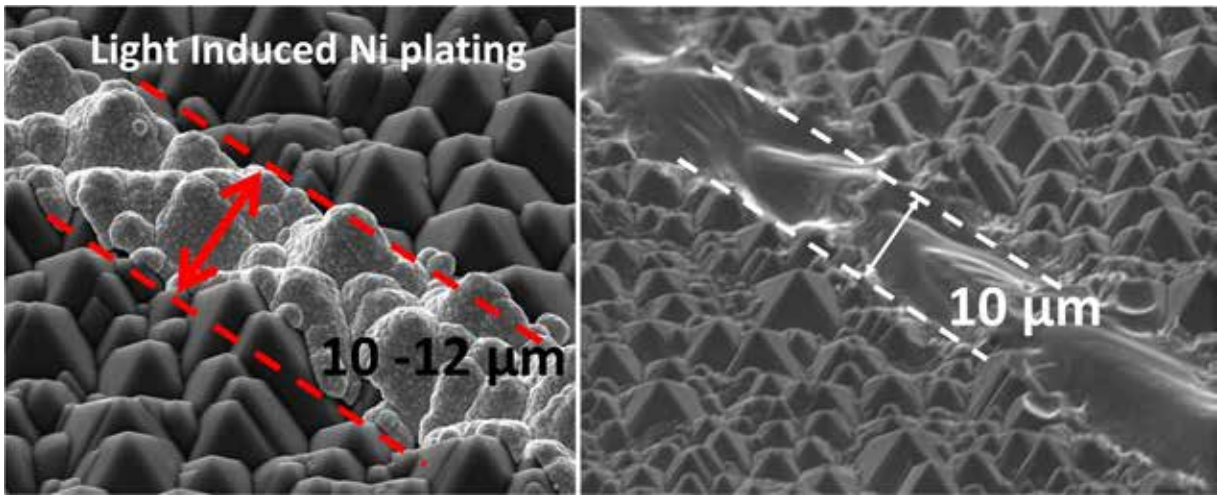

Figure 4. SEM images showing the surface finishing on the front side for (a) a laser-ablated and nickel-plated device, and (b) a laser-doped cell.

Process flow	R_{sheet} FSF [Ω/sq.]	FSF patterning	Rear passivation	J_{sc} [mA/cm^2]	V_{oc} [mV]	*FF* [%]	Efficiency [%]
1	120	Laser ablation	SiO_2	39.4	668	80.9	21.3*
2	120	Laser ablation	Al_2O_3	39.1	677	81.3	21.5**
3	250	Laser doping	Al_2O_3	39.9	684	80.7	22**

*Internal measurements; **Measurements performed at FhG ISE CalLab.

Table 1. *I–V* results from imec's n-PERT devices after the implementation of the specified optimized features.

doping and metal plating is the optimal combination for a simple process for high-efficiency contact formation. The final width of the front fingers after plating is between 25 and 30µm wide.

Thanks to the use of selective laser doping, a higher resistive FSF is integrated in the devices (R_{sheet} ≈ 250–300Ω/sq.). The passivated J_0 for this lightly doped FSF is ~25fA/cm^2. After laser doping and annealing, $J_{0,laser}$ values below 3000fA/cm^2 were measured; this results in an implied V_{oc} of more than 690mV.

Cell results

Table 1 summarizes imec's top-efficiency cells obtained over the past two years with a diffused n-PERT structure, along with their main differences. All the process flows have the following in common: n-type Cz wafers with a thickness around 160µm and a base resistivity between 3 and 5Ωcm were used to manufacture the devices. The front side is textured with an alkaline solution, resulting in random pyramids with a front reflection down to 9.5% at 700nm (before ARC). The front dielectrics consist of a thin thermal oxide used for the passivation of the FSF, and a PECVD SiN_x layer used as the ARC. The standard diffused rear emitter implemented in all the flows features an R_{sheet} of ~90–100Ω/sq. The rear dielectrics are patterned by laser ablation, and a 2µm PVD AlSi layer is used as a rear electrode. Finally, after laser patterning and metallizing the front of the cells, the edges are isolated for carrying out the electrical characterization.

Flow 1 was based on thermal oxide passivation on both front and rear surfaces, single diffusion for the FSF formation, and laser ablation for the front-side patterning. Average efficiencies over 21% were achieved with this sequence; the V_{oc} was limited to ~668mV by both the front and the rear recombination.

The use of Al_2O_3 as the rear passivation in flow 2 led to increases in V_{oc} and *FF*, which in turn led to a 0.2% abs. increase in efficiency compared with that for the SiO_2 passivated reference. The optimization of the FSF (by combining it with selective laser doping), the Al_2O_3 passivation on the rear emitter, and the improved front optics and an optimized front metallization collectively resulted in a record, independently confirmed efficiency of 22%.

The expected increase in implied V_{oc} observed for the high-resistivity emitter with selective laser doping is also seen for the devices from flow 3. The increase in J_{sc} results from a combination of different aspects: the optimization of the ARC and texturing steps, the improved blue response with the lightly doped FSF, and a modification of the front-metallization pattern. Further experiments are necessary to understand the decrease in *FF* for flow 3 as compared to flow 2.

Other paths to achieving even higher efficiencies are under investigation – for example a modification of the front metallization through the implementation of SmartWire Connection Technology [13].

Light-induced degradation (LID)

Using the devices corresponding to flow 2 in Table 1, the impact of the light illumination on the n-PERT devices was evaluated and compared

with a p-type PERC reference. It was observed that after 12h of illumination at one sun, the n-PERT cells did not show any signs of degradation, whereas the p-type PERC reference cells showed a loss of ~3mV in V_{oc} and 2% in *FF*. It is therefore confirmed that imec's n-PERT devices do not suffer from LID.

"Independently confirmed efficiencies of 22% have been achieved for large-area devices with imec's current process flow."

Conclusion

The main features of imec's n-PERT cells have been presented in this paper. An optimization of the main features of the devices on test structures has been demonstrated and the devices evaluated at the cell level. Of particular interest was the combination of the selective junction formation by laser doping and the self-aligned front metallization by Ni/Cu plating. Independently confirmed efficiencies of 22% have been achieved for large-area devices with imec's current process flow, and a clear path towards realizing 22.5% has been described.

References

[1] Metz, A. et al. 2014, "Industrial high performance crystalline silicon solar cells and modules based on rear surface passivation technology", *Solar Energy Mater. & Solar Cells*, Vol. 120, Part A, pp. 417–425.

[2] Osborne, M. 2015, "Trina solar starts PERC technology volume production", News Report (Jan. 19th) [http://www.pv-tech.org/news/trina_solar_starts_perc_technology_volume_production].

[3] Recaman, M. et al. 2014, "Opportunities for silicon epitaxy in bulk crystalline silicon photovoltaics", *Proc. 29th EU PVSEC*, Amsterdam, The Netherlands.

[4] Tous, L. et al. 2015, "Process simplification in large area hybrid silicon heterojunction solar cells", *Proc. 5th SiliconPV*, Konstanz, Germany.

[5] SEMI PV Group Europe 2014, "International technology roadmap for photovoltaic (ITRPV): Results 2013", 5th edn (Mar.) [http://www.itrpv.net/Reports/Downloads/].

[6] Cornagliotti, E. et al. 2014, "Large area n-type c-Si solar cells featuring rear emitter and efficiency beyond 21%", *Tech. Digest 6th WCPEC*, Kyoto, Japan.

[7] Hoex, B. et al. 2007, "Excellent passivation of highly doped p-type surfaces by negative-charge-dielectric Al_2O_3", *Appl. Phys. Lett.*, Vol. 91, p. 112107.

[8] Duerinckx, F. et al. 2014, "Quantifying internal optical losses for 21% n-Si rear junction cells", *Proc. 29th EU PVSEC*, Amsterdam, The Netherlands.

[9] Aleman, M. et al. 2014, "Reducing front recombination losses to improve the efficiency of rear junction Cu-plated n-Si cells", *Proc. 29th EU PVSEC*, Amsterdam, The Netherlands.

[10] Hallam, B. et al. 2013, "Deep junction laser doping for contacting buried layers in silicon solar cells", *Solar Energy Mater. & Solar Cells*, Vol. 113, pp. 124–134.

[11] Hallam, B. et al. 2014, "Hydrogen passivation of laser-induced defects for silicon solar cells", *IEEE J. Photovolt.*, Vol. 4, No 6, pp. 1413–1420.

[12] Uruena, A. et al. 2015 [forthcoming], "Beyond 22% large area n-type silicon solar cells with front laser doping and a rear emitter", *Proc. 30th EU PVSEC*, Hamburg, Germany.

[13] Meyer Burger 2014, "SmartWire Connection Technology", White Paper [http://www.meyerburger.com/en/media/downloads/publications/].

About the Authors

Monica Aleman received her mechanical engineering degree in Venezuela in 2003 and her Ph.D. in micro-electronics in 2013 from Freiburg University, Germany. She has worked on Si solar cells since 2004 and first focused on front metallization while at Fraunhofer ISE. Monica has been at imec since 2009, where her main interest is the development of high-efficiency n-type cells.

Angel Uruena is a silicon PV research scientist at imec, where he focuses on the development of n-type solar cells. He obtained a B.Sc. in telecommunications and an M.Sc. in electronics in 2004 and 2007 respectively, from the University of Valladolid. Angel then received his Ph.D. in electrical engineering in 2013 from KU Leuven.

Emanuele Cornagliotti received his M.Sc. in 2006 from the Politecnico of Torino, Italy, and his Ph.D. in electrical and electronic engineering in 2011 from KU Leuven, Belgium. Since 2007 Emanuele has been a researcher at imec, working on the development of industrial silicon solar cells, with a focus on process integration.

Aashish Sharma received his B.Sc. in physics from Jacobs University Bremen in 2010 and his M.Sc. in optics and photonics from Karlsruhe Institute of Technology in 2012. Aashish is currently pursuing a Ph.D. at imec and KU Leuven, working on high-efficiency n-PERT c-Si solar cells.

Richard Russell received a bachelor's in physics from the University of Exeter, England, and a master's in physics from the University of Dundee, Scotland. Between 1990 and 2010 he worked for BP Solar, mainly on Ni/Cu-metallized laser-grooved buried contact cells. In 2011 Richard joined imec, where he leads copper-based metallization activities within the iPERx platform.

Filip Duerinckx leads the iPERx platform in the silicon photovoltaics group at imec. He received his M.Sc. in engineering from KU Leuven, Belgium, in 1994, followed by his Ph.D. in 1999. Filip's current focus is on performance and economic aspects of n-type PERx silicon solar cells.

Jozef Szlufcik received his M.Sc. and Ph.D. degrees, both in electronic engineering, from the Wroclaw University of Technology, Poland. He joined imec in 1990 as head of research on low-cost crystalline silicon solar cells, and then from 2003 to 2012 held the position of R&D and technology manager at Photovoltech, Belgium. Jozef is currently the director of the photovoltaics department at imec.

Enquiries

Monica Aleman
imec
Kapeldreef 75
B-3001 Leuven
Belgium

Tel: +32 16 28 78 55
Email: Monica.Aleman@imec.be